

A Modified Approach to Crossing Number and Post-processing Algorithms for Fingerprint Minutiae Extraction and Validation

Iwasokun Gabriel Babatunde*
Akinyokun*
Oluwole Charles*
Alese Boniface Kayode*

Abstract

Fingerprint has remained a very vital index in the field of security where series of Automatic Fingerprint Identification System (AFIS) have been developed for human identification. Many of these systems involve matching each of the features of a template image with each of the features in the feature sets in the reference database to determine the level of match between the template and the reference images. Matching is done on the basis of preset parameters such as feature type, location, orientation and so on. Obtaining the features from the template image and for building a reference database involves the implementation of a sound fingerprint feature detection and extraction algorithm. In this paper, the process of detecting and extracting false and valid features contained in a fingerprint image is discussed. Some of the existing fingerprint features extraction algorithms were firstly modified and the resulting algorithms were implemented. The implementation was carried out in an environment characterized by Window Vista Home Basic as platform and Matrix Laboratory (MatLab) as frontend engine. Fingerprints images of different qualities obtained from the manual (ink and paper) and electronic (fingerprint scanner) methods were used to test the adequacy of the resulting algorithms. The results obtained show that valid minutiae points were extracted from the images.

Keyword: AFIS, Pattern recognition, pattern matching, fingerprint, Post processing, Minutiae extraction

1. Introduction

In the world today, fingerprint is an essential index used in the enforcement of security and maintenance of a reliable identification of any individual. Fingerprint is currently being used as variables of security during voting, operation of bank accounts among others. It is equally used for controlling access to highly secured places like offices, equipment rooms, control centers and so on. The following reasons had been adduced for the wide use and acceptability of fingerprint for the enforcement of security [1-4]:

- a. Fingerprints have a wide variation since no two people have identical prints.
- b. Unlike in other biometrics, fingerprints exhibit high degree of consistency and they do not change in relative appearance.
- c. Fingerprint is left each time the finger contacts a surface.

Other reasons for the much larger market of personal authentication using fingerprints are:

- a. Availability of small and inexpensive fingerprint capture devices
- b. Availability of fast computing hardware
- c. High recognition rate devices that meet the needs of many applications

- d. The explosive growth of network and Internet transactions
- e. The heightened awareness of the need for ease-of-use as an essential component of reliable security.

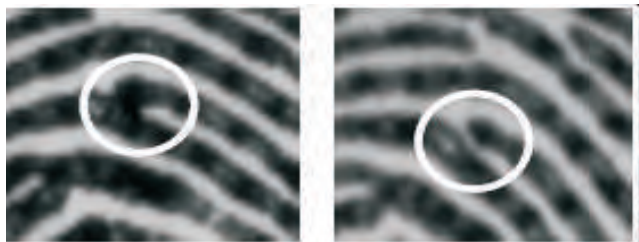
2 Fingerprint Features

The main ingredients of any fingerprint that are useful during pattern recognition and matching tasks are its features. The features are defined by type, position, orientation and so on and they exhibit uniqueness from fingerprint to fingerprint. Fingerprint features are classified into two categories; namely local and global features [5]. The local features are the tiny, unique characteristics of fingerprint ridges that are used for identification. They are found in the local area only and are invariant with respect to global transformation [6]. Two or more impressions of same finger may have identical features but still differ because they have minutia points that are different [7]. In Figure 2.1, ridge patterns (a) and (b) are two different impressions of the same finger (person). The same minutia point is read as bifurcation in (a) while it appears as a ridge ending in (b).

Global features are characterized by the attributes that capture the global spatial relationships of a fingerprint. The following are the common fingerprint global features [7-9]:

2.1 Basic Ridge Patterns:

The ridge patterns are the patterns formed from the dark areas of the finger tip epidermis produced when a finger is pressed against a smooth surface. The valleys are the bright areas. Ridges and valleys run in parallel as shown in Figure 2.2. The ridges form pattern of left loop, right loop, whorl, arch and tented arch as shown in Figure 2.3. In the loop pattern, the ridges enter from either side, re-curve and pass out or tend to pass out the same side they entered. In the right loop pattern, the ridges enter from the right side while the ridges enter from the left side in the left loop. In a whorl pattern, the ridges are usually circular while in the arch pattern, the ridges enter from one side, make a rise in the center and exit generally on the opposite side.



(b) Minutiae as a bifurcation point

(a) Minutiae as an end point

Figure 2.1: The same minutiae extracted from two different impressions.

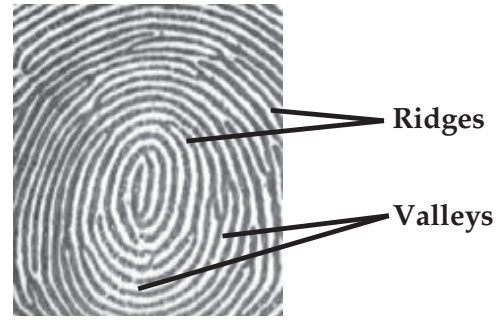


Figure 2.2: Ridges and valleys on a fingerprint image



Figure 2.3: Basic types of fingerprint pattern

2.2 Pattern Area

The pattern area is the part of the fingerprint where the global features are found. Fingerprints can be read and classified based on the information in this area. The following are the information that are available in the pattern area of a fingerprint [2-4]:

- a. **Type:** Different types of minutiae are found in the fingerprint pattern area. They include termination, bifurcation, lake, independent ridge, point or island, spur, cross over and so on.
- b. **Orientation:** The minutia orientation is defined by the direction of the minutia point. The orientations of the ridge ending and bifurcation of Figure 2.4 are marked as θ and β respectively.
- c. **Spatial Frequency:** Spatial frequency refers to how far apart the ridges are in the neighborhood of the minutia point. It is measured by the average distance apart of the ridges.
- d. **Curvature:** The curvature refers to the rate of change of ridge orientation. The curvature, c of one of the two ridge endings of Figure 2.5 is obtained from the absolute difference between θ_2 of Figure 2.5(b) and θ_1 of Figure 2.5(a). It is the displacement angle resulting from the change in orientation of the ridge pattern.

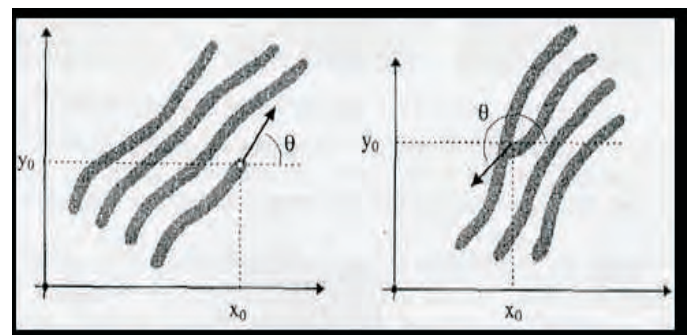


Figure 2.4: Minutia point orientation

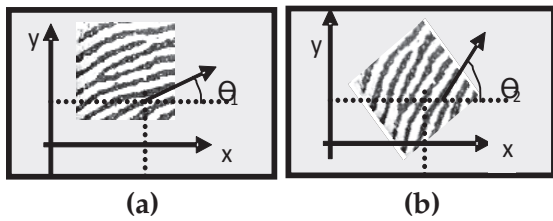


Figure 2.5: Change in ridge orientation

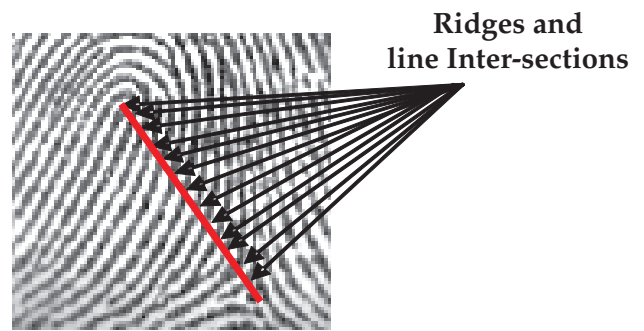


Figure 2.6: The ridge count between delta and core

- e. **Position:** The position of the minutia point refers to its x, y location, either in an absolute sense or relative to fixed points like the Delta and Core points.
- f. **Core and Delta Areas:** The core area is located at the approximate center of the finger impression as shown in Figure 2.6 and it is used as a reference point for reading and classifying the print. The Delta area is the region in the ridge pattern where there is triangulation or a dividing of the ridges as shown in Figure 2.6. It is also the point of the first bifurcation, abrupt ridge ending, meeting point of two ridges, dot, fragmentary ridge, or any point upon a ridge at or nearest to the center of divergence of two type lines, located at or directly in front of their point of their point of divergence. It is a definite fixed point used to facilitate ridge counting and tracing.
- g. **Type Lines and Ridge Count:** Type Lines are the two innermost ridges that start parallel, diverge, and surround or tend to surround the pattern area. When there is a definite break in a type line, the ridge immediately outside that line is considered to be its continuation. The Ridge Count is most commonly the number of ridges between the Delta and the Core. To establish the ridge count, an imaginary line is drawn from the Delta to the Core and each ridge that touches this line is counted. The ridge count between the core and delta shown in Figure 2.7 is the number of ridges crossed by the imaginary lines drawn across the ridges.



Figure 2.6: The Delta and Core structure of fingerprint

3. Feature Detection and Extraction

The detection and extraction of features in a fingerprint image is next to the image enhancement stage. In [10-11], several image enhancement algorithms were discussed and implemented. Features were also detected and extracted from the thinned images obtained as the final results of the enhancement stage. A Crossing Number (CN) method for feature detection and extraction from the thinned image had been implemented in [12-13]. In the CN method, the extraction of the features is done through the scanning of the 3 x 3 neighbourhood of each ridge pixel in the thinned image. The CN value is then calculated from half the sum of the differences between pairs of adjacent pixels in the eight-neighbourhood as shown in Equation 3.1.

$$CN = 0.5 \sum_{i=1}^8 |P_i - P_{i+1}|, \quad P_9 = P_1 \quad \dots \dots 3.1$$

Using the CN properties shown in Table 3.1, the ridge pixel is classified as a ridge ending, bifurcation or non-minutiae point. For example, a ridge pixel with a CN of one corresponds to a ridge ending, a CN of 2 corresponds to a continuing ridge point and a CN of three corresponds to a bifurcation.

Table 3.1
Properties of the Crossing Number.

CN	Property
0	Isolated point
1	Ridge end point
2	Continuing ridge point
3	Bifurcation point
4	Crossing point

Similar to the Crossing number approach was the method proposed in [14-15]. These authors devised a method that uses a 3 x 3 window to examine the local neighbourhood of each ridge pixel in a skeleton image. A pixel is classified as a ridge ending if it has only one neighbouring ridge pixel in the window, and classified as a bifurcation if it has three neighbouring ridge pixels. False minutiae may be introduced into the image due to factors such as noisy images, and image artifacts created by the thinning process [12]. Hence, after the extraction of minutiae, it is important that a post-processing method is employed to validate the minutiae. Some examples of false minutiae structures are

illustrated in Figure 3.1. The false structure include the spur, hole, triangle and spike structures [16]. From inspection, it is revealed that the spur structure generates false ridge endings, while both the hole and triangle structures generate false bifurcations. The spike structure on its own generates a false bifurcation and a false ridge ending point.

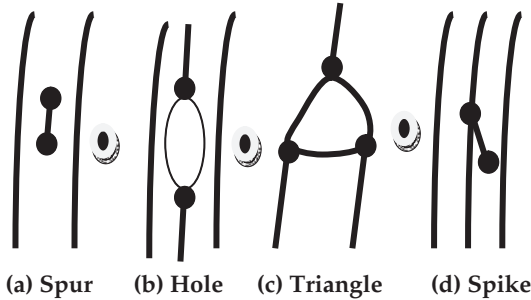


Figure 3.1: Examples of typical false minutiae structures.

A novel approach to the validation of minutiae is the post-processing algorithm proposed in [17]. This algorithm operates on the skeleton image. However, rather than employing a different set of heuristics each time to eliminate a specific type of false minutiae, this approach incorporates the validation of different types of minutiae into a single algorithm. It tests the validity of each minutiae point by scanning the skeleton image and examining the local neighbourhood around the minutiae. The algorithm is able to cancel out false minutiae based on the configuration of the ridge pixels connected to the minutiae point. In this research, the Crossing Number (CN) method for a pixel P is slightly modified with a view to speed up its operation. The modified version is presented as follows:

$$CN = \sum_{j=0}^7 |P_{j+2} - P_{j+1}|, \quad P_9 = P_1 \quad \dots \dots 3.2$$

The eight neighbouring pixels of P are scanned in clockwise direction as follows:

P ₂	P ₃	P ₄
P ₁	P	P ₅
P ₈	P ₇	P ₆

With this modification, a ridge pixel with CN of 2 corresponds to ridge ending and CN of 6 corresponds to bifurcation as shown in Figure 3.2. Towards ensuring that only valid minutiae are extracted, a minutiae validation algorithm proposed in [17] was also modified before its implementation. The modified algorithm tests the validity of each minutiae point by scanning the skeleton image and examining the local neighbourhood around the point. The first step in the algorithm is the creation of an image M of size W x W centered on the candidate minutiae point in the skeleton image. The central pixel of M is labelled with a value of -1. The rest of the pixels in M are initialised to values of zero, as shown in Figure 3.3(a) and Figure 3.3(d).

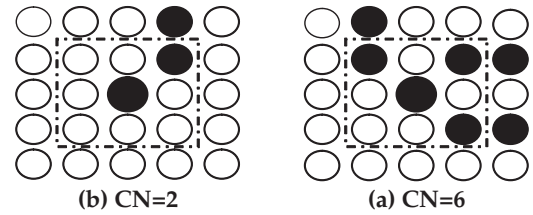


Figure 3.2: CN values for ridge ending and bifurcation point

The subsequent steps of the algorithm depend on whether the candidate minutiae point is a ridge ending or a bifurcation.

- i. For a candidate bifurcation point:
 - Examine the 3 x 3 neighbourhood of the bifurcation point in a clockwise direction. For the three pixels that are connected with the bifurcation point, label them with the value of 1. An example of this initial labelling process is shown in Figure 3.3(b).
 - Label with 1 the three ridge pixels that are connected to these three connected pixels. Examples of this labelling process is shown in Figure 3.3(c).
 - Count in a clockwise direction, the number of transitions from 0 to 1 (T01) along the border of image M. If T01 = 3, then the candidate minutiae point is validated as a true bifurcation.
- ii. For a candidate ridge ending point:
 - Label with a value of 1 all the pixels in M, which are in the 3 x 3 neighbourhood of the ridge ending point (Figure 3.3(e)).
 - Count in a clockwise direction, the number of 0 to 1 transitions (T01) along the border of image M. If T01 = 1, then the candidate minutiae point is validated as a true ridge ending.

4. Experimental Results

The fingerprint minutiae extraction experiment was carried out in an environment characterized by Window Vista Home Basic Operating System as platform and MatLab (Matrix Laboratory) as frontend engine on a Pentium IV Personal computer with 1.87GB processor and 1024MB RAM. The essence of the experimental stage is to ascertain that the modified CN and the post-processing algorithms perform well like their initial versions in the detection and extraction of features from fingerprint images. Shown Figures 4.1(a) and (b) are the results of using the modified CN method to extract minutiae from a medium quality fingerprint image obtained using a manual fingerprinting method. Figures 4.1 (c) and (d) show the results for the fingerprint image obtained from the electronic method. From the experimental plots of the extracted minutiae points on the thin images shown in Figure 4.1(a) and 4.1(c), it is deduced that both the true and false ridge pixels corresponding to a CN value of two and six have been detected from the images. Ridge endings are denoted by six pointed stars (hexagrams), and bifurcations are denoted by diamonds. The experimental plot presented in Figure 4.1(b) and Figure 4.1(d) depict the extracted false and true minutiae points superimposed on the original image. Visual inspection of the plots on the images indicates that the majority of the marked minutiae points from the thin images correspond to valid minutiae points in the original images. In all the plots, false minutiae point sets are covered by large boxes with appropriate labels.

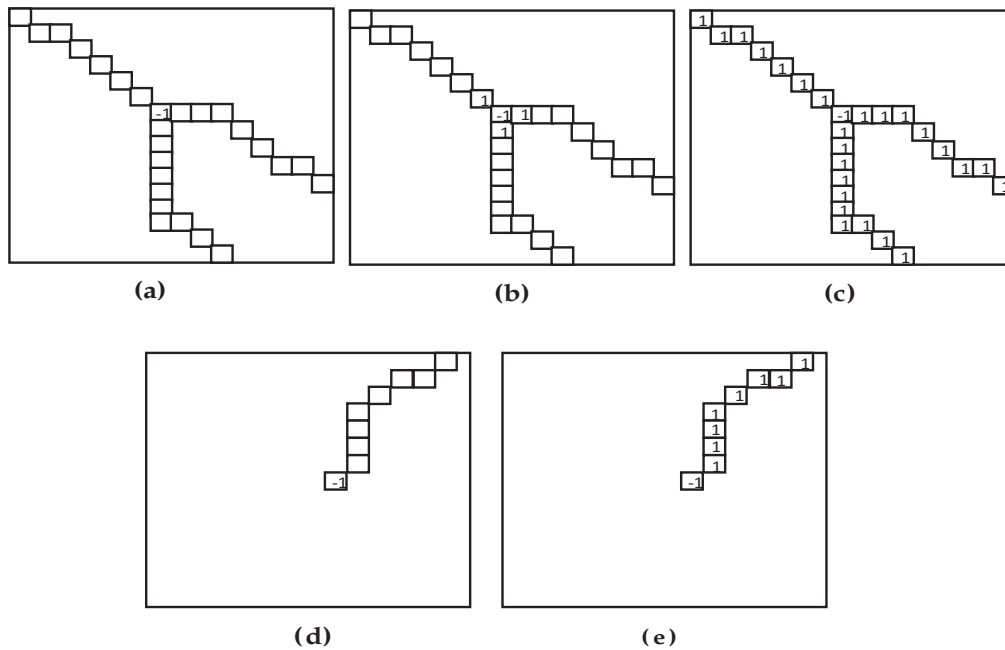


Figure 3.3: Example of validating a candidate bifurcation point $T_{01}=3$ and ridge ending point. $T_{01} = 1$.

Enlarged views of the false minutiae points shown in Figures 4.1 (a) and (b) are presented in Figure 4.2. Figure 4.2(a) depicts a false minutiae point called a cross-over structure, which corresponds to the box labeled 1 and Figure 4.2(b) depicts a false minutiae point comprising of both the hole and the spike structures, which correspond to the box labeled 2. It can be seen that the cross-over structure shown in Figure 4.2(a) generates two false bifurcation points while the hole and spike structures shown in Figure 4.2(b) generate two false bifurcation points and a false end point. Similarly, the spike structure shown in Figure 4.2(c) generates two false endpoints. However, in the original image shown in Figure 4.1(b), these minutiae points do not exist. The modified post-processing algorithm was implemented to eliminate the false minutiae that were extracted using the modified CN method. The experimental plots of the result of the post-processing experiment on the images shown in Figure 4.1 are presented in Figure 4.3. It is revealed in Figure 4.3(a) and Figure 4.3(c) that all the false minutiae points on the skeleton images have been eliminated at the post-processing stage.

The results shown in Figure 4.3 were obtained with image window of size 25×25 centered on the candidate minutia point. When window size is smaller than this value, the algorithm could not eliminate some false minutiae points. Shown in Figure 4.4(a) and Figure 4.4(b) are the false minutiae points not eliminated due to small window size of 21. This is due to fact that the entire local neighbourhood around the candidate minutiae points could not be captured. This forced the number of 0 to 1 transition to 3 for bifurcation as illustrated in Figure 3.3(c). The number of 0 to 1 transition is also forced to 1 for the ridge ending as illustrated in Figure 3.4(b). Similarly with a higher window size, the algorithm eliminated some valid minutiae points. Shown in Figure 4.4(c) is the valid minutia point that is eliminated due to oversize window of 29. This is explaining the fact that the window extended beyond the local neighbourhood of the candidate minutia point and hence the number of 0 to 1 transition round the border is forced to 0.

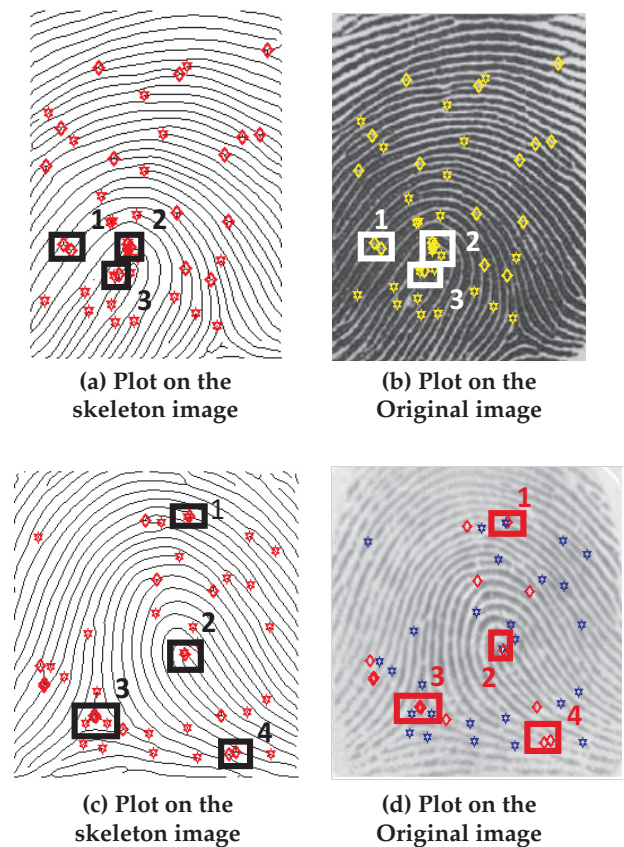


Figure 4.1: Results of performing minutiae extraction on a fingerprint image obtained by manual and electronics methods.

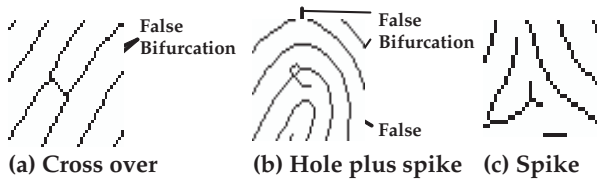


Figure 4.2: Enlarged view of the false minutiae from Figure

5. Conclusion

The research being reported in this paper is a verification of the previously concluded research works of other authors. The CN method proposed and implemented in [12-13] had been modified by varying the order and reducing the level of computation. The post-processing algorithm proposed in [17] was modified by labelling all the three connecting ridges to the candidate bifurcation point with 1 thereby raising the 0 to 1 transition to 3. The modified algorithms were implemented with images obtained from the manual (ink and paper) method as well as the electronic (fingerprint scanner) method. In the manner of the original algorithm, the modified CN algorithm extracted both the false and true minutiae points from the fingerprint images. Results also show that with suitable window size, the modified post-processing algorithm extracted all the true minutiae points from the images and ignored all the false minutiae points.

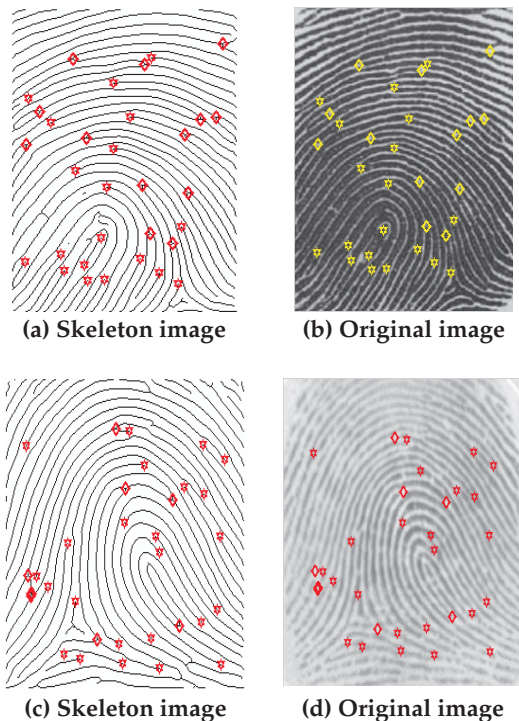


Figure 4.3: Results of minutiae post-processing experiment

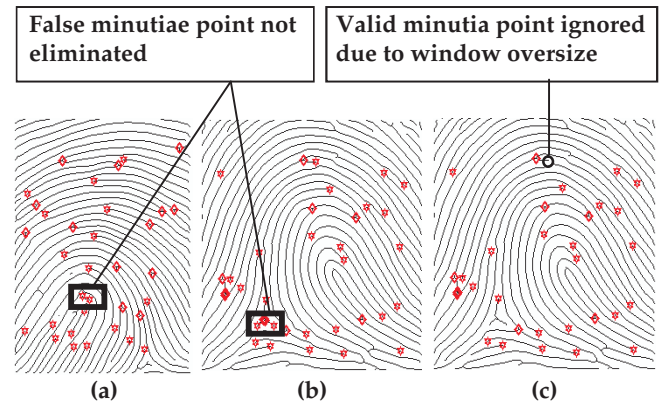


Figure 4.4: Experimental plots for too small and too large neighbourhood

6. References

1. C. Roberts). 'Biometrics' (<http://www.ccip.govt.nz/newsroom/information-notes/2005/biometrics.pdf>. Accessed 23rd May, 2009
2. M. Cherry and E. Imwinkelried. "A Cautionary Note About Fingerprint Analysis and Reliance on Digital Technology", *Public Defense Backup Center REPOR Volume XXI Number 3 T*, 2006, pp7-9
3. M. J. Palmiotto. 'Criminal Investigation'. Chicago: Nelson Hal, 1994, pp234-239
4. D. Salter. 'Fingerprint – An Emerging Technology', *Engineering Technology, New Mexico State University*. 2006
5. O. C. Akinyokun and E. O. Adegbeyeni. 'Scientific Evaluation of the Process of Scanning and Forensic Analysis of Fingerprints on Ballot Papers', *Proceedings of Academy of Legal, Ethical and Regulatory Issues*, Vol. 13, Numbers 1, New Orleans, 2009:
6. L. Hong, Y. Wan and A. K. Jain. 'Fingerprint image enhancement: Algorithm and performance evaluation'. *IEEE Transactions on Pattern Analysis and Machine Intelligence* 20, 8, 2001, pp 777-789.
7. J. Tsai-Yang and V Govindaraju. 'A minutia-based partial fingerprint recognition system', *Center for Unified Biometrics and Sensors, University at Buffalo, State University of New York, Amherst, NY USA 14228*, 2004
8. D. Stoney. 'Measurement of fingerprint individuality'. *Advances in Fingerprint Technology*, 2nd Ed. By Henry C Lee, R. E Gaensslen, CRC Press, 2001
9. E. O. Adegbeyeni and O. C. Akinyokun. 'Techno Legal Issues of Scanning and Forensic Analysis of Ballot Papers Fingerprints'. *Federal University of Technology, Akure, Nigeria*, 2008.
10. J. Tsai-Yang and V. Govindaraju. 'A minutia-based partial fingerprint recognition system'. *Pattern Recognition*. Vol. 38, 10, 2006, pp. 1672-1684.
11. L. Hong, Y. Wan and A. Jain. 'Fingerprint image enhancement: Algorithm and performance evaluation'; *Pattern Recognition and Image Processing Laboratory, Department of Computer Science, Michigan State University*, 2006, pp1-30
12. T. Raymond. 'Fingerprint Image Enhancement and Minutiae Extraction', *PhD Thesis Submitted to School of Computer Science and Software Engineering, University of Western Australia*, 2003, pp21-56.
13. N. Sara, D. Sergie and V. Gregory 'User Interface Design of the Interactive Fingerprint Recognition (INFIR) System', 2004

14. A. K. Jain, L. Hong, S. Pankanti, and R. Bolle. "An identity authentication system using fingerprints". *Proc. IEEE*, 85(9), 1997, 1365–1388.
15. N. Ratha, S. Chen and A. K. Jain 'Adaptive Flow Orientation Based Feature Extraction in Fingerprint Images', *Pattern Recognition*, Vol. 28, No. 11, 1995, pp 1657-1672.
16. Q. Xiao and H. Raafat. 'Pattern Recognition', 24,10, 1991, pp985-992
17. M. Tico and P. Kuosmanen. 'An algorithm for fingerprint image postprocessing', *Proceedings of the Thirty-Fourth Asilomar Conference on Signals, Systems and Computers*, vol. 2, 2000, pp. 1735–1739.